Journal of Applied Polymer Science

Effect of the dissolution time on the structure and properties of lyocell-fabric-based all-cellulose composite laminates

Bapan Adak, Samrat Mukhopadhyay
Department of Textile Technology, Indian Institute of Technology Delhi, Hauz Khas, New Delhi 110016, India
Correspondence to: S. Mukhopadhyay (E-mail: samrat@textile.iitd.ac.in)

ABSTRACT: In this study, all-cellulose composite laminates were prepared from lyocell fabric with ionic liquid (1-butyl-3-methyl imidazolium chloride), a conventional hand layup method, and compression molding. Eight layers of lyocell fabric, which were impregnated with ionic liquid, were stacked symmetrically and hot-pressed under compression molding for various times; this resulted in the partial dissolution of the surface of the lyocell fibers. The dissolved cellulose held the laminas together and resulted in a consolidated laminate. Finally, the prepared laminate was impregnated in water to remove the ionic liquid and to regenerate a matrix phase *in situ;* this was followed by hot-press drying. Optical microscopy and scanning electron microscopy studies were used to analyze composite structures. With increasing dissolution time, the void content in the composites decreased, and the interlaminar adhesion improved. For LC-2h and LC-3h, the highest tensile strength and modulus values obtained were 48.2 MPa and 1.78 GPa, respectively. For LC-4h, the highest flexural strength and modulus values obtained were 53.96 MPa and 1.2 GPa, respectively. © 2016 Wiley Periodicals, Inc. J. Appl. Polym. Sci. **2016**, *133*, 43398.

KEYWORDS: cellulose and other wood products; composites; ionic liquids; mechanical properties; structure–property relations

Received 29 June 2015; accepted 4 January 2016
DOI: 10.1002/app.43398

INTRODUCTION

Nowadays, worldwide environmental awareness has restricted the use of many biocomposites where nonbiodegradable petroleum-based material are used as the matrix phase.[1] Therefore, research efforts have currently been directed toward the development of a new class of fully biodegradable green composites through the combination of natural/biofibers with biodegradable matrices, such as poly(lactic acid), polyhydroxybutyrate, and poly[3-hydroxybutyrate-*co*−3-hydroxyvalerate].[2] However, there is still the issue of compatibility between the hydrophobic polymer matrix and hydrophilic biofibers as reinforcements in biocomposites.[3] This problem has been minimized to a great extent by the physical or chemical modification of the fibers/matrix,[4–6] but more research is still required in this field.

Recently, an alternate approach has been developed to prepare environmentally friendly composites, so-called single-polymer composites, which are based on an ecodesign concept.[7] In addition to the success of single-polymer-based all-polypropylene composites or all-polyethylene composites, fully cellulose-based all-cellulose composites (ACCs) are also becoming very popular by the day. Because of the chemical similarity of the matrix and reinforcing phase, these are able to overcome the problem of poor fiber–matrix adhesion.[8]

ACCs are one of the latest class of single-polymer composites, where both the matrix and reinforcing phase are based on cellulose. Cellulose is currently the most abundantly available biopolymer in the world.[8,9] Moreover, the low density, high strength, and biodegradability of cellulosic fibers add to the advantages for its use in biocomposites as reinforcements.[4,8] The main components of plant-based cellulosic fibers are cellulose, hemicellulose, lignin, pectin, waxes, and water. However, natural biofibers are nonuniform, and their quality and mechanical properties may vary, depending on the different growing conditions, fiber extraction procedures, and maturity of the harvested plant.[10] The presence of lignin and hemicellulose in lignocellulosic biofibers (jute, sisal, ramie, bagasse, etc.) may be an obstacle to the preparation of an effective ACC because of the poor solubility of these constituents in cellulosic solvents under the used process conditions.[8] Therefore, the use of regenerated-cellulose-based fibers such as viscose, modal, and lyocell can redress this problem with the achievement of good properties in the ACCs, as these fibers offer greater consistency in terms of the mechanical properties, fiber structure, and fiber diameter when compared with natural fibers.[11] On the basis of the possibility of developing different forms (film/sheet/laminate) and having good promising properties, ACCs may find many potential applications, ranging from biomedical to structural applications, in the near future.

In this study, lyocell fabric (3:1 twill weave) was used to produce ACC by partial dissolution or a surface selective dissolution technique with a simple hand-layup process with compression molding. An ionic liquid (1-butyl-3-methyl imidazolium chloride) was used as the solvent; it fell into the class of so-called green solvents and had a very low vapor pressure, nontoxicity, nonflammability, good thermal stability, and easy recyclability.[12,13] The changes in the structure and properties of the manufactured composites as a function of the dissolution time are discussed.

EXPERIMENTAL

Materials

An ionic liquid (1-butyl-3-methyl imidazolium chloride) was used as a cellulose solvent and was purchased from Sigma Aldrich. Lyocell fabric (3:1 twill) with GSM-210, EPI-76, and PPI-62 was supplied by Aditya Birla Group, and it was used as a starting material for the synthesis of ACC. The lyocell fabric had basic strengths of about 33 and 26.1 MPa in the warp and weft directions, respectively. It had breaking extensions of about 23 and 26.4% in the warp and weft directions, respectively. The lyocell fiber was composed of pure regenerated cellulose, mainly in the form of cellulose II, and it had a crystallinity of about 67%. Deionized water was used as a nonsolvent to regenerate cellulose.

Material Preparation

The ionic liquid was heated in a vacuum drier at 105 °C for 24 h before use to remove residual moisture. The lyocell fabric was initially washed in hot water (80 °C) to remove water-soluble sizes and other impurities from the fabric and then dried at room temperature. Then, it was cut to 18 × 15 cm^2 and dried in a vacuum drier for 90 min at 90 °C before we used it for composite preparation.

Composite-Laminate Preparation

The dried lyocell fabric was impregnated in the preheated ionic liquid and spread evenly on the fabric with a plastic scraper to produce a single lamina. Eight layers of these laminas were stacked symmetrically, with warp yarns of all fabric pieces kept in the same direction. It was placed between two aluminum foils and folded on three sides, with one side kept open to collect excess ionic liquid when pressed. The whole foil-based system containing the laminas was subsequently placed under a compression-molding machine, where it was pressed at 110 °C. The dissolution times in compression molding were varied at 30 min, 1 h, 2 h, 3 h, and 4 h with the pressure kept constant (1 MPa).

Then, the hot-pressed consolidate laminates were impregnated in distilled water for 24 h. In between, water was exchanged four times for the complete removal of the ionic liquid from the laminates. Subsequently, the regenerated laminates were dried by hot pressing at 0.1 MPa of pressure at 100 °C for 30 min and then at 80 °C for 2 h. The steps of composite preparation are schematically illustrated in Figure 1.

Testing and Characterization

Wide-angle X-ray diffraction patterns of lyocell fabric and corresponding laminates were obtained with a PaNalytical PW3040

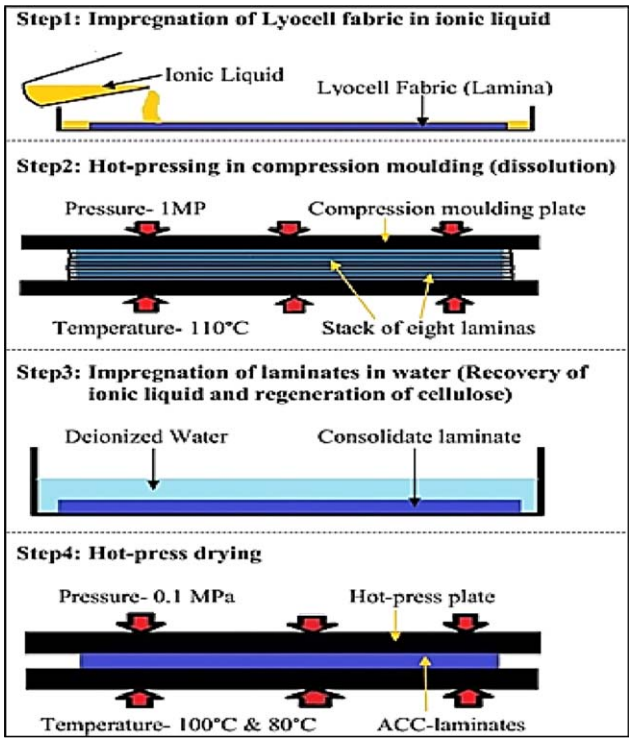

Figure 1. Schematic diagram of the steps for the preparation of lyocell ACCs. [Color figure can be viewed in the online issue, which is available at wileyonlinelibrary.com.]

X'Pert Pro (The Netherlands) X-ray diffractometer with Cu Kα radiation ($\lambda = 1.54$) with 40 kW of power and 30 mA of current. The $2\ominus$ range was set from 10 to 40° at a rate of 0.04°/s, where $\ominus$ is Bragg's angle. The X-ray diffraction profiles were analyzed with Peak Fit software, where the diffraction profiles were resolved into noncrystalline (amorphous) scattering and crystalline reflections. The percentage crystallinity ($\%X_C$) was measured with the following equation:

$$\%X_C = \sum A_c / \sum A_t \quad (1)$$

where $\sum A_t$ is the total area (crystalline plus amorphous) under the graph and $\sum A_c$ is the only crystalline area under the graph.

The surfaces of the ACC laminates and lyocell fabric were observed with a polarized optical microscope (Nikon SMZ1500, Japan). All of the samples were analyzed with 30× magnification.

The cross-sectional binding and the tensile-fractured surfaces of the ACCs were observed with scanning electron microscopy (SEM). Initially, the composite samples were dried for 24 h at 80 °C to make them moisture free and cut to a size of 8 mm (length) by 3 mm (width) with a circular saw cutter. The samples were further placed on conductive carbon black tape and sputtered coated with gold with 25 mA of current. SEM was performed with a Zeiss Evo 18 (Special Edition) instrument with an accelerating voltage of 20 kV.

The thickness of the lyocell fabric and ACCs were measured with a slide caliper associated with the Vernier scale with an accuracy level up to 0.02 mm (Mitutoyo, Japan). At least 10

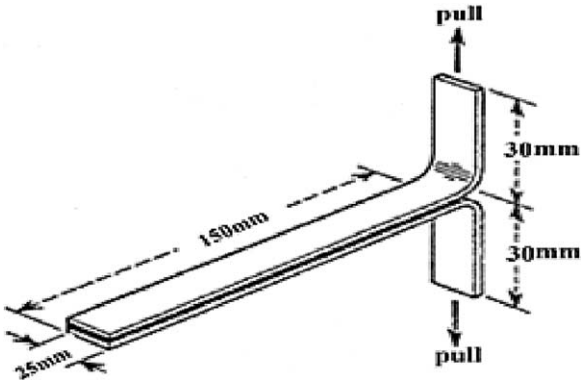

Figure 2. T-peel test specimen.

readings were taken for each sample, and the average values are reported.

For density measurement, the samples were cut to a particular size (2 × 2 cm^2). Then, for each samples, we calculated the average thickness (in centimeters) by measuring the thickness in 10 different places. The volume (V) of each sample was calculated with this equation:

$$V(\mathrm{cm}^3) = \text{Length} \times \text{Width} \times \text{Thickness} \quad (2)$$

Here, Length = Width = 2 cm. Then, the weight (W) in grams was noted from the weighing balance for each composite sample, and the apparent density (D_a) of the composites were measured with the following equation:

$$D_a = W/V \quad (3)$$

The bulk density (D_b) of the regenerated-cellulose-based lyocell fiber was assumed to be about 1.52 g/cc.[14,15] The percentage void content (%V) in the composites was calculated with the following equation:

$$\%V = [1-(D_a/D_b)] \times 100\% \quad (4)$$

The T-peel test was carried out according to ASTM D 1876-08 with a Tinius Olsen universal testing machine. A 25 mm wide strip was cut from each composites, torn off at one end, as shown in Figure 2 (T-type specimen) and peeled off at a constant velocity of 254 mm/min. The machine was equipped with suitable grips capable of firmly clamping the specimens without slippage throughout the tests. During the peel test, the applied load was recorded in a graph as a function of the distance peeled (in millimeters). To calculate the peel strength, the mean of the recorded peak loads was used and divided by the width of the peeled stripe. For each composites, eight samples were tested.

The tensile properties of the prepared ACCs were measured by a method from ASTM D 3039. As the thickness of samples were varied from 1.5 to 1.9 mm, the samples were cut into a size of 150 mm (in length) by 8–10 mm (in width) for tensile testing. The samples were tested in an Instron 4301 tensile tester with a 5-kN load cell. The test was performed with a crosshead speed of 2 mm/min and a gauge length of 40 mm. All samples were conditioned for 24 h at a 65 ± 2% relative humidity and 20 ± 2 °C before tensile testing. The direction along the warp yarns in the lyocell fabric was considered as the longitudinal direction of ACCs.

Flexural tests were performed at room temperature with the three-point bending method according to ASTM D 790-10. A Zwick Z010 flexural testing machine was used for this purpose. Specimens 60 mm in length and 12.7 mm in width were cut and loaded into the three-point bending tester with a recommended span-to-thickness ratio of 16:1. The specimens were tested at a crosshead speed of 2 mm/min. The flexural stress was noted against the displacement up to 15 mm for each sample. The flexural strength and flexural modulus were calculated with eqs. (8) and (9), respectively[16]:

$$\sigma = (3FL)/(2bt^2) \quad (5)$$

$$E = (L^3 m)/(4bt^3) \quad (6)$$

where F is the maximum load (N), L is the support span (mm), b is the width of the sample (mm), t is the thickness of the samples (mm), m is the slope of the initial straight line portion of the load–deflection curve, σ is the flexural strength (MPa), and E is the flexural modulus (MPa).

RESULTS AND DISCUSSION

Wide-Angle X-ray Diffraction Analysis

Figure 3 shows the X-ray diffraction profiles for the lyocell fabric and lyocell ACCs. The regenerated-cellulose-based lyocell fiber could have a mixture of cellulose II and cellulose III crystal structures,[17] whereas under certain conditions, the formation of cellulose IV was also favored.[18,19] For lyocell fabric, a weak peak was found at $2\ominus = 12°$ (plane 101), and two almost indistinguishable peaks were found at $2\ominus = 22°$ (plane 002) and 20.6° (plane 021). The peaks at $2\ominus = 12$ and 22° were mainly for cellulose II, whereas the peak at $2\ominus = 20.6°$ may have been due to the presence of cellulose III.[20] The partial dissolution of the lyocell fabric and the regeneration of dissolved cellulose was accompanied by a change in the diffraction peak from 20.6° to a lower value 19.8° with a gradual reduction in the peak

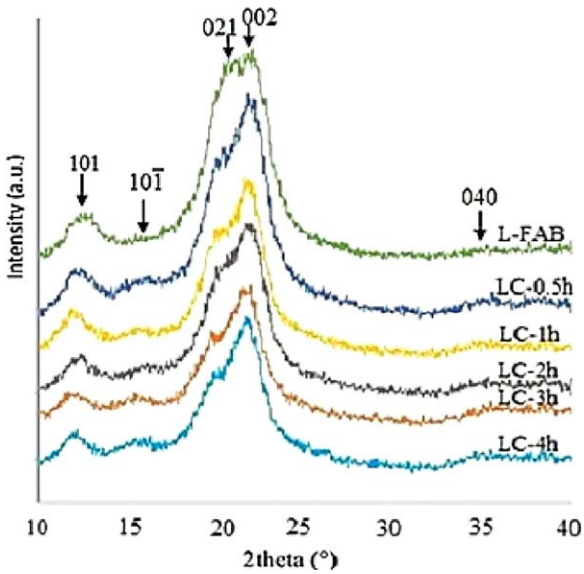

Figure 3. X-ray diffraction profiles for the lyocell fabric and lyocell ACCs. [Color figure can be viewed in the online issue, which is available at wileyonlinelibrary.com.]

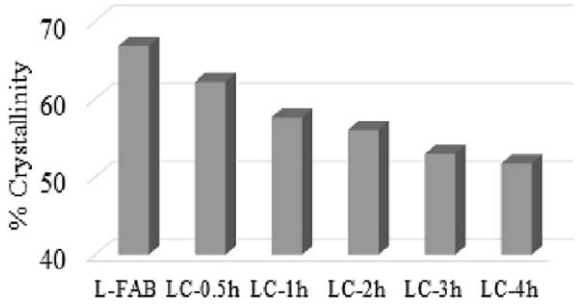

Figure 4. Crystallinity (%) of the lyocell fabric and ACCs produced with various dissolution times.

intensity with increasing dissolution time. The peak for the lyocell fabric at $2\ominus = 12°$ shifted to a slightly lower $2\ominus$ value in the case of lyocell ACCs. Although there was no peak at $2\ominus = 16°$ in the X-ray diffraction profile of the lyocell fabric, a new peak was observed at about $2\ominus = 16°$ (plane 101) for the lyocell ACCs. This peak may have been due to the presence of cellulose I or cellulose IV.[21] However, cellulose II is more stable than cellulose I because of the antiparallel packing of cellulose chains in cellulose II[22] and does not transform into cellulose I.[8,21] This indicates that the peak at $2\ominus = 16°$ for the lyocell ACCs was possibly due to presence of cellulose IV_{II}, which might have been formed from cellulose II caused by heating during dissolution and drying.[8,19,23]

The crystallinity of the as-received lyocell fabric was about 66.8%, and because of this high crystallinity, it took longer for the proper dissolution of the lyocell fibers. From the X-ray diffraction patterns, it was clear that with increasing dissolution time, the intensity of the peaks (at planes 021 and 002) decreased gradually; this indicated a reduction in the crystallinity of the ACCs because of the breaking of intermolecular and intramolecular hydrogen bonds between cellulose molecules during the dissolution process.[24] Figure 4 shows the graphical representation of $\%X_C$ values for the lyocell fabric and ACCs. We observed that at a higher immersion time, more cellulose was dissolved, and it formed a less oriented and less crystalline or paracrystalline regenerated matrix phase. This resulted in a reduction in the overall crystallinity of the ACCs,[25,26] as shown in Figure 4.

Surface Morphology of the Lyocell ACCs

Figure 5 shows the surface images of the lyocell fabric and ACCs under an optical microscope with 30× magnification; this shows the effect of time on the dissolution of cellulose. From these images, it is clear that with increasing time, because of the increase in cellulose dissolution, the pores or voids that were present in the fabric (between yarn interstices) and among the layers were gradually filled up by dissolved cellulose. This resulted in a comparatively smoother surface in the ACCs. In Figure 5(A), which was recorded from the gray lyocell fabric, sharp twill lines were clearly visible. With increasing dissolution time, the sharpness of twill line diminished gradually in the ACCs because of the increased partial dissolution of the lyocell fiber surface. The surface color of the prepared ACCs changed from white (in the fabric) to slightly brownish (in ACC) after the treatment with IL for a longer time. This may have been due to the slight degradation of cellulose for processing at high temperatures for prolonged times.[13,27]

Cross-Sectional Binding of Lyocell ACCs

Figure 6 shows the SEM micrographs for the cross-sectional view and interlaminar bonding in different lyocell ACCs. These images show that the process resulted in extensive interlaminar and intralaminar bonding with the formation of minimum voids with higher dissolution times. With increasing dissolution time, the intralaminar and interlaminar voids were reduced significantly and led to improved interfacial adhesion between the regenerated matrix and the undissolved cellulose fraction. In the case of LC-0.5h, although the dissolved cellulose was able to bind the undissolved part, the individual yarns were clearly visible in the composite cross section [Figure 6(A,B)]. With 1- and 2-h dissolution times, improved adhesion was observed as a result of the further dissolution of cellulose. However, still fabric layers could be clearly identified in the cross sections of LC-1h and LC-2h; they showed lines in the fiber–matrix interface. With higher dissolution times (3 and 4 h), almost no distinct interface was found; this justified the term *interfaceless composite*.[23]

Thickness, Apparent Density, and Void Content

The lyocell fabric used here as a basic material for ACC preparation had a thickness of about 0.46 mm. However, the ACCs generated in this process were several millimeters in thickness; they varied between 1.47 and 1.91 mm, depending on the process conditions. We observed that initially, with increasing dissolution time, the thickness of the ACCs decreased because of a greater dissolution of cellulose and the application of high pressure. However, after 2 h of dissolution, almost no more change was observed in the thickness of the lyocell ACCs (Table I).

For the 30-min dissolution time, the void content in the lyocell composite (LC-0.5h) was very high (ca. 36%) because of the large interlaminar and intralaminar void spaces in the composite. However, with increasing dissolution time, the void content in the lyocell ACCs gradually decreased as the void were filled up by more dissolved cellulose. A minimum void content value of 3.4% was obtained for the ACC produced with 4 h of dissolution time. On the contrary, the apparent density of the composites gradually decreased with increasing dissolution time because of the reduction in the void content and the increase in the compactness.

Mechanical Properties

Peel Strength. The peel strength is the average strength per unit width of the bond line required to produce progressive separation of two bonded, flexible adherents. It is a measure of the interlaminar adhesion strength. Figure 7 shows that with increasing dissolution time, the peel strength of the lyocell composites gradually increased; this demonstrated the increased interlaminar adhesion of the ACCs. We observed that the peel strength increased 12-fold when the dissolution time increased from 30 min to 4 h. The lyocell ACC produced with 4 h of dissolution time showed an average peel strength of about 2.96 N/mm, which was superior even to those of metalized carbon fiber-reinforced epoxy composites[28] and E-glass fabric reinforced

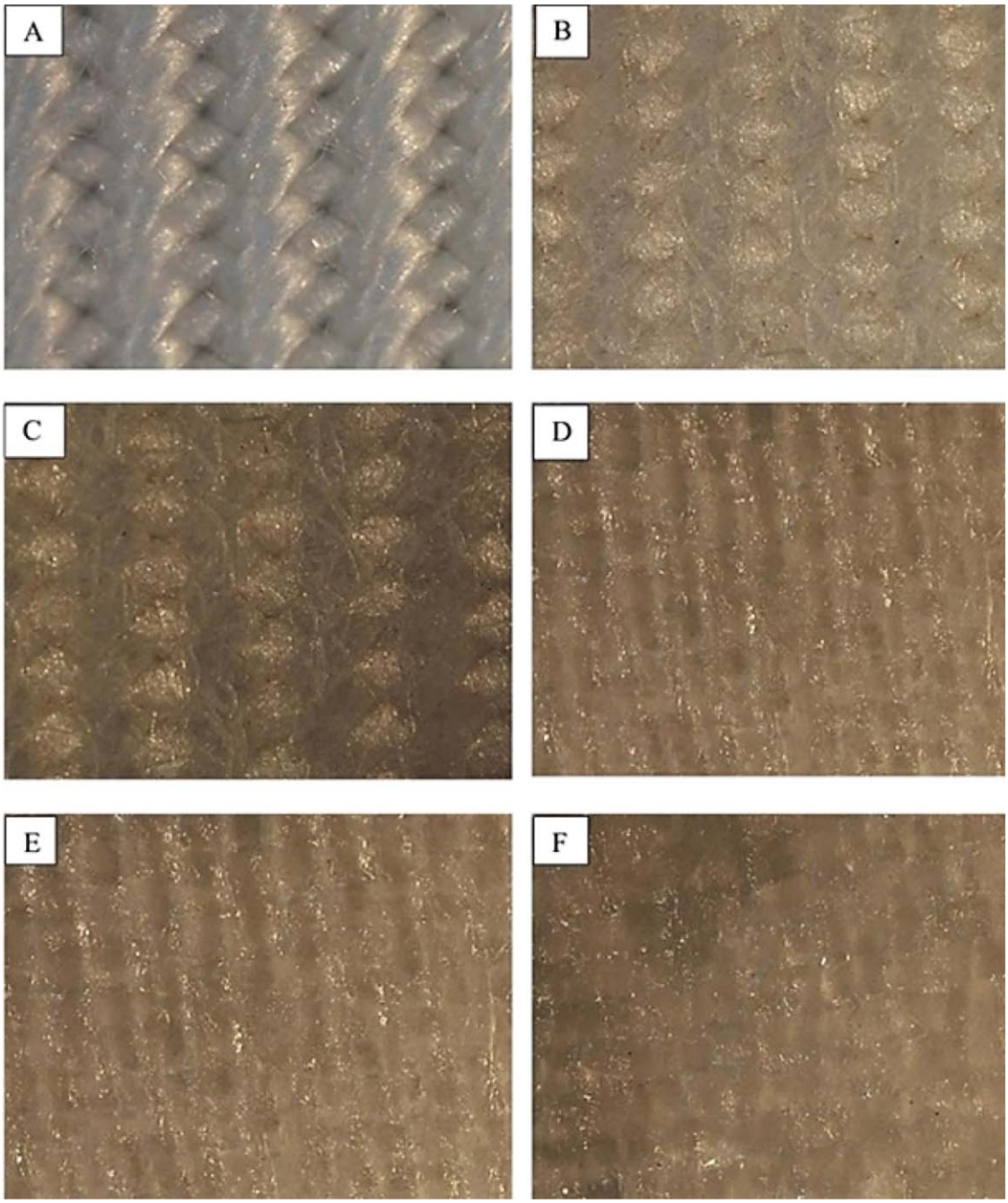

Figure 5. Optical microscopy images of the surfaces of the lyocell fabric: (A) Lyocell fabric (L-FAB) and (B–F) lyocell composites (LC-0.5h, LC-1h, LC-2h, LC-3h, and LC-4h, respectively; magnification = 30×). [Color figure can be viewed in the online issue, which is available at wileyonlinelibrary.com.]

polyester composites.[29] This high interlaminar adhesion in the lyocell ACCs was due to the chemical similarity and high compatibility of the matrix and reinforcing phase.[30,31]

Tensile Properties. The tensile properties of the lyocell ACCs were found to be a function of the basic structure of the lyocell fibers and process conditions. In general, lyocell fibers possess a skin–core structure. However, they are less porous and more oriented than regenerated-cellulose-based viscose fibers.[19] The structure of lyocell fibers may also change, depending on the process conditions and composition of the regeneration bath during fiber manufacturing.[17] The lyocell fiber used here was manufactured with a regenerating bath containing N-Methylmorpholine N-oxide (NMMO) and water. Abu-Rous and coworkers[32,33] observed the cross section of a similar type lyocell fiber using transmission electron microscopy, where the fiber cross section contained a compact core, a porous middle zone, and a semipermeable fiber skin. The cellulose dissolution and the ultimate mechanical properties of the lyocell ACCs were solely dependent on the structure of these lyocell fibers.

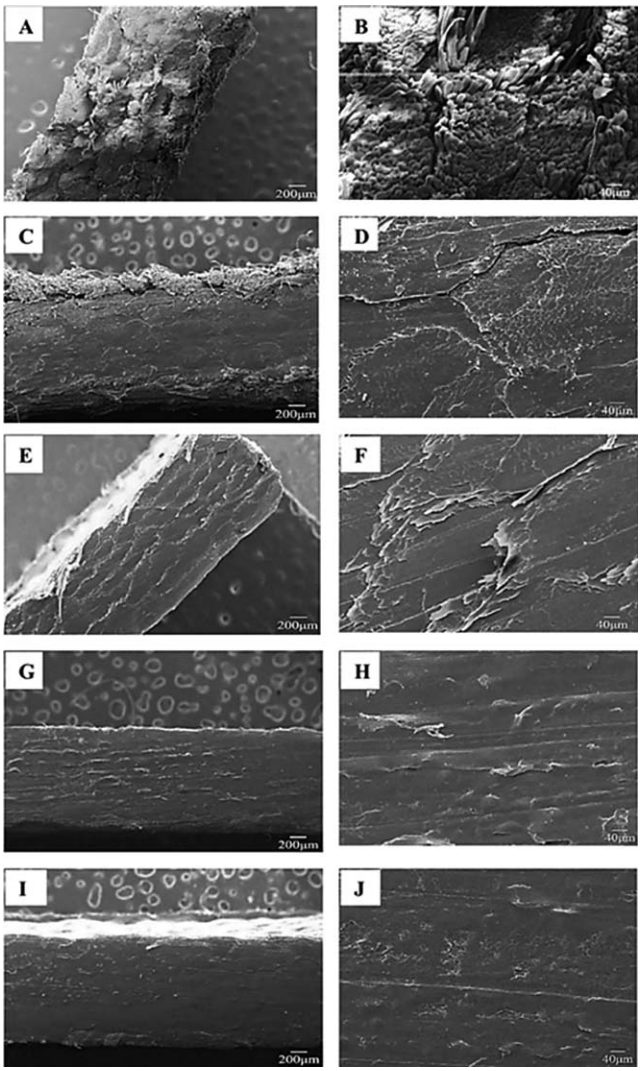

Figure 6. SEM micrographs with lower (50×) and higher magnification (300×) of (A,B) LC-0.5h, (C,D) LC-1h, (E,F) LC-2h, (G,H) LC-3h, and (I,J) LC-4h.

Figure 8 shows the tensile properties of ACCs developed in this study; this highlighted the effect of the dissolution time. With increasing dissolution time, two contradictory effects played a significant role in controlling the tensile strength of the lyocell ACCs: (1) more dissolution of cellulose caused a reduction in the strength of the basic cellulosic material, and (2) an increase

Table I. Thickness, Apparent Density, and Void Content Values of the Lyocell ACCs

Sample	Thickness (mm)	Apparent density (g/cm^3)	Void content (%*V*)
LC-0.5h	1.91 ± 0.03	0.97	36.06
LC-1h	1.8 ± 0.02	1.09	28.39
LC-2h	1.49 ± 0.04	1.32	13.03
LC-3h	1.47 ± 0.02	1.46	4.08
LC-4h	1.48 ± 0.02	1.47	3.39

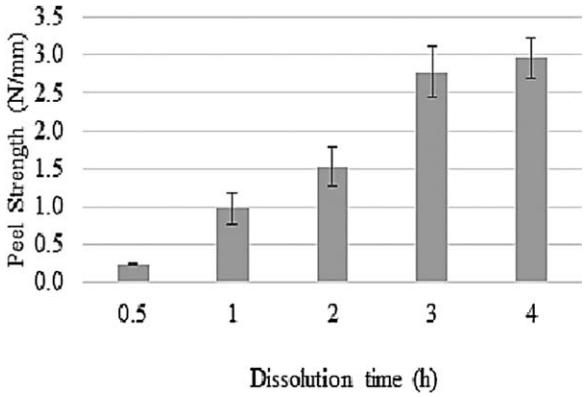

Figure 7. Change in the peel strength of the lyocell ACCs produced with various dissolution times.

in amount of dissolved cellulose helped to form a sufficient matrix and finally resulted in an improved fiber–matrix adhesion and, consequently, an increase in the composite strength.

The longitudinal tensile strength of the lyocell composites increased up to 2 h because of the formation of an efficient matrix phase through the dissolution of the top skin and

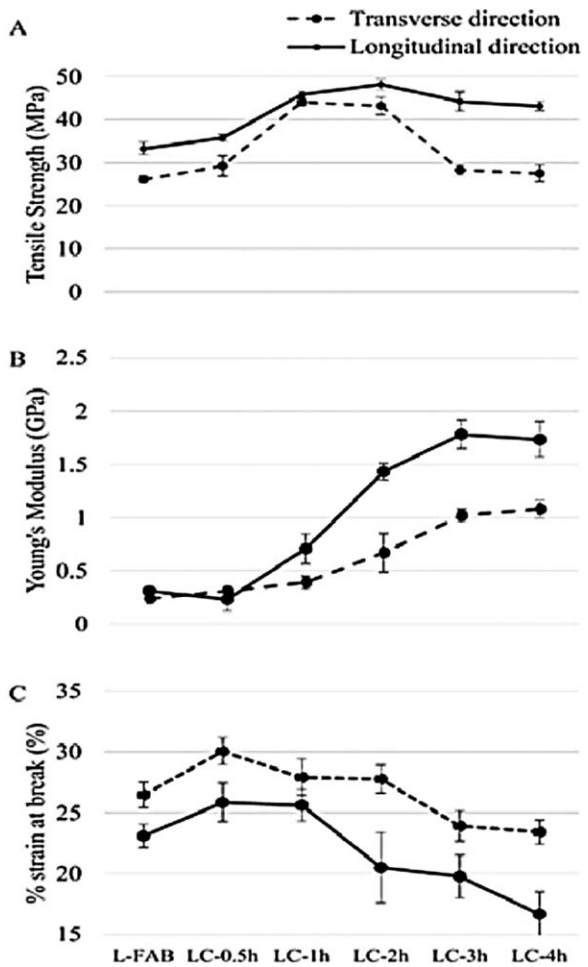

Figure 8. Tensile properties of the lyocell ACCs produced with various dissolution times.

porous middle section of the lyocell fibers. This resulted in better stress transfer between the matrix and undissolved cellulose reinforcement. The highest tensile strength achieved was 48.2 MPa for LC-2h. After 2 h, because of a higher amount of cellulose dissolution, the core part of the lyocell fibers also dissolved, and this affected the basic strength of the lyocell fibers.[25] This resulted in a decrease in the tensile strength of the composites produced with higher dissolution times (3 and 4 h). However, in the transverse direction, the tensile strength of the lyocell ACCs continuously dropped with increasing dissolution time after 1 h for the same reason [Figure 8(A)].

Because the basic material for these composites was in fabric form, good tensile properties were obtained in both the longitudinal and transverse direction. The tensile strength of the lyocell-based ACCs varied between 35 and 48 MPa in the longitudinal direction and between 29 and 44 MPa in the transverse direction. In comparison to the transverse direction, the higher strength in the longitudinal direction was due to difference in the basic strengths of the lyocell fabric in the warp and weft directions. However, the transverse strength obtained here was far superior to other ACCs, as was previously reported in other literature.[25,34]

The Young's modulus of the lyocell ACCs continuously increased with increasing dissolution time [Figure 8(B)]. The presence of voids had a crucial impact on the Young's modulus of the ACCs.[35] With increasing dissolution, the intralaminar and interlaminar voids had a tendency to decrease; this resulted an increase in the Young's modulus or stiffness of the lyocell ACCs. The ACCs processed for 3 h (LC-3h) had a stiffness that was more than seven times higher than that of the ACCs produced with 30 min of dissolution time (LC-0.5h). However, after 3 h, no further increase in the stiffness was noticed, and actually, it decreased slightly for the 4-h processing time.

The modulus in the transverse direction followed an almost similar trend. However, the lyocell ACCs possessed a slightly lower modulus in the transverse direction than they did in longitudinal direction.

The percentage strain at break (%ε) initially increased for the ACC produced with 30 min of dissolution time. After that, it decreased continuously because of the increase in stiffness with increasing dissolution time [Figure 8(C)]. The longitudinal %ε value for LC-0.5h was about 25.9%; this became almost half after 4 h of processing (for LC-4h). The breaking strain in the transverse direction varied in a similar fashion to the longitudinal direction with increasing dissolution time. In fabric, because of the interlacement between the warp and weft, crimps were created in the crossover points. On the other hand, generally, a higher crimp is noticed in weft direction of fabric compared to the warp direction because of comparatively higher stress in the warp direction during fabric manufacturing.[36,37] This may be the major reason behind the observation that the lyocell fabric and the fabric-based ACCs showed a comparatively higher %ε and a lower stiffness in the transverse direction than they did in the longitudinal direction.

Repeatability of the Tensile Properties of the Lyocell ACCs. Figure 9 shows the repeatability of the tensile properties in the longitudinal direction of the lyocell ACCs produced with various dissolution times. This graph proves that the processes showed a great repeatability in terms of all of the tensile properties (strength, modulus, and breaking extension). The values of the achieved tensile properties were not only almost the same; it followed nearly the same trend with various dissolution times.

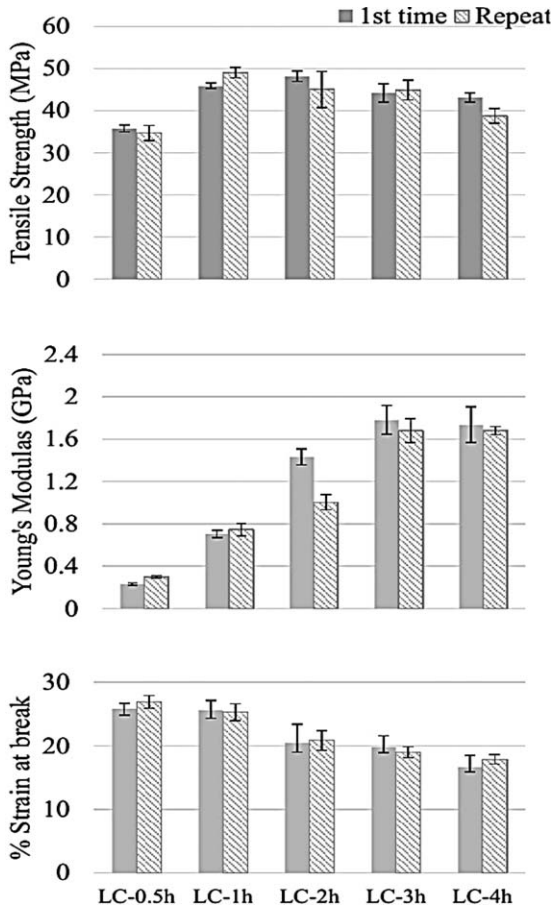

Figure 9. Repeatability of the tensile properties of the lyocell ACCs produced with various dissolution times.

Tensile-Fractured Behavior. The tensile-fractured samples of the lyocell ACCs processed with various dissolution times are shown in Figure 10. The main tensile-fractured modes observed were fiber/yarn breakage, fiber/yarn pullout, and delamination of individual fabric layers; this was been marked in the SEM images of the fractured surface for different lyocell ACCs (Figure 11). For the ACCs produced with lower dissolution times (30 min and 1 h), the tensile failure was mainly due to the delamination of fabric layers and fiber/yarn breakage, whereas individual yarns showed little or no adhesion to neighboring yarns [Figure 11(A,B)]. The composite LC-0.5h did not even rupture completely, and failure was only due to delamination, as shown in Figure 10(A). These types of failure were due to the lack of bonding between adjacent laminas/yarns/fibers and suggested the formation of an inadequate matrix phase to bind the reinforcement. However, for a higher dissolution time, as the fiber–matrix adhesion improved, the ACCs became stiffer. So, a slightly ductile-type fracture with little delamination and

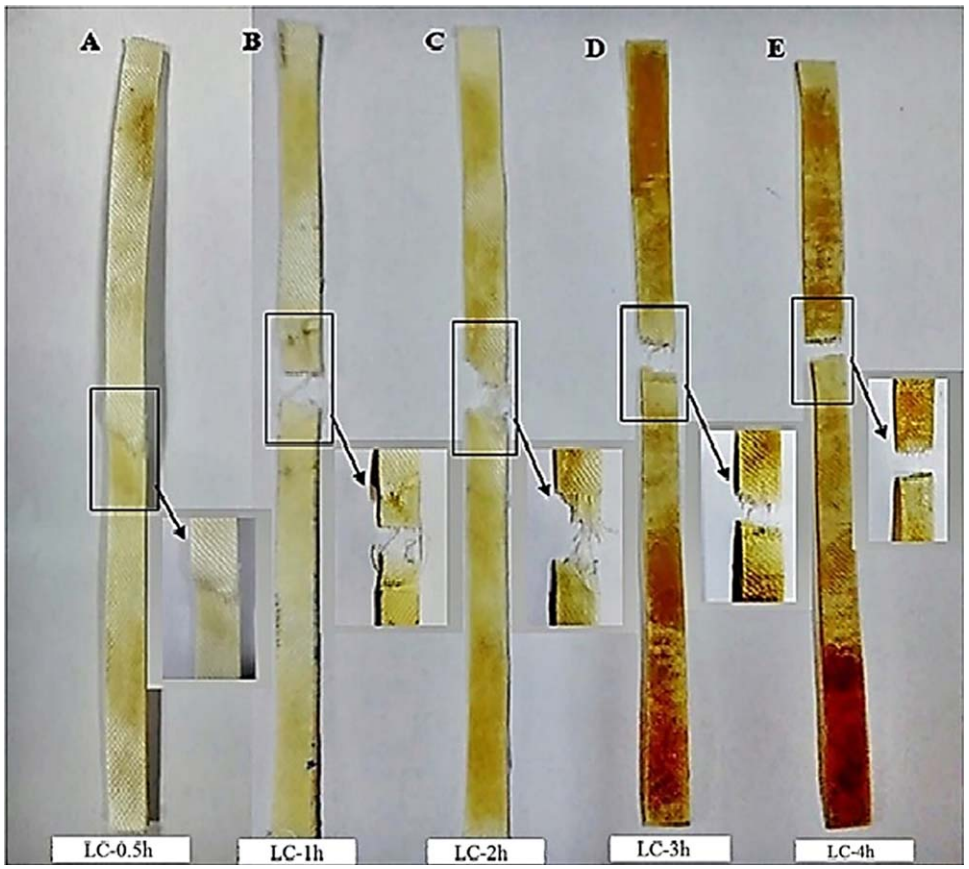

Figure 10. Tensile-fractured samples of the lyocell ACCs produced with various dissolution times. [Color figure can be viewed in the online issue, which is available at wileyonlinelibrary.com.]

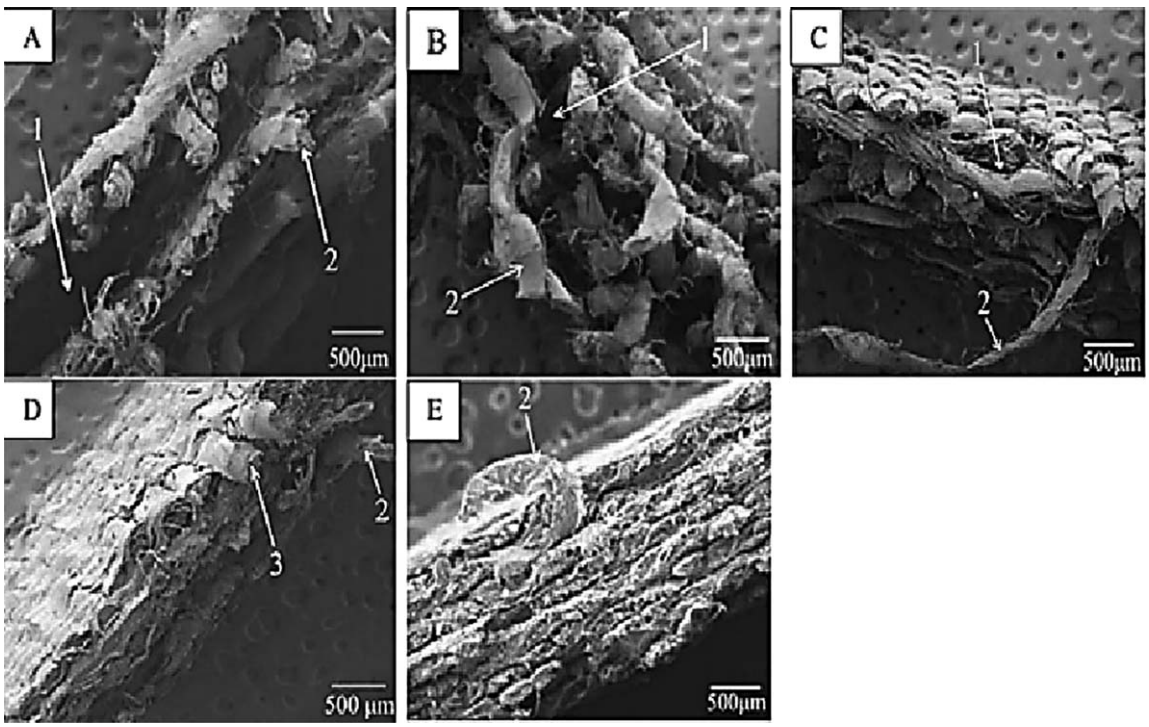

Figure 11. SEM micrographs of the tensile-fractured surfaces of the lyocell ACCs with a magnification of 80×: (A) LC-0.5h, (B) LC-1h, (C) LC-2h, (D) LC-1h, and (E) LC-4h. The different fracture modes were the (1) delamination of layers, (2) pulled-out yarn, and (3) fractured yarn.

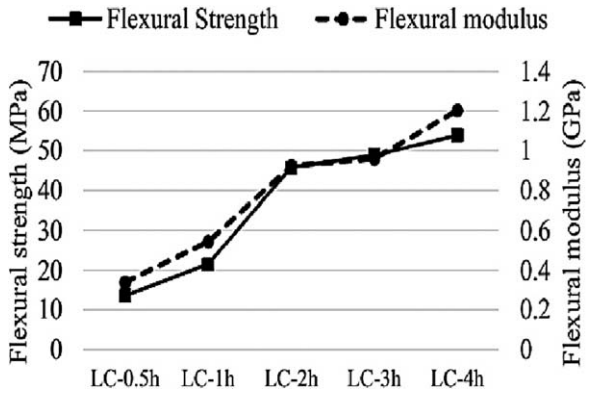

Figure 12. Flexural strength and modulus values of different lyocell ACCs.

comparatively lower fiber/yarn pullout was observed for the ACCs produced with 2 h of dissolution time [Figure 10(C)].

The tendency of the delamination gradually decreased with increasing dissolution time as a result of better intralaminar and interlaminar adhesion. Therefore, for LC-3h and LC-4h, comparatively lower pullouts of the fibers/yarns were observed [Figure 11(D,E)]; this indicated slightly brittle-type fracture.

Flexural Properties. The flexural strength is the ability of a material to withstand bending forces applied perpendicular to its longitudinal axis, whereas the flexural modulus is a measure of the resistance to deformation in bending.[38] During flexural testing, the materials can be subjected to tensile, compressional, and shear stresses, which produce a compound stress together.[39]

The flexural properties of the lyocell ACCs are shown in Figure 12, as an effect of the dissolution time. Both the flexural strength and modulus increased with increasing dissolution time; this revealed that ACCs produced with higher dissolution times could withstand bending forces to a great extent. This was due to the formation of better interfacial adhesion between the undissolved part of the lyocell fabric and the regenerated matrix. Similar to the tensile properties, the interlaminar and intralaminar voids played important roles in controlling the flexural properties, especially the flexural modulus.[35] With increasing dissolution time from 30 min to 4 h as the internal voids gradually decreased, consequent rises in the flexural strength and modulus were observed by 4 times and 3.5 times, respectively. The highest flexural strength and modulus were achieved for LC-4h, and the values were 54 MPa and 1.2 GPa, respectively. This might have been due to the presence of the lowest void content and the better fiber–matrix adhesion compared to those of the other ACCs. The obtained flexural strength for the LC-3h and LC-4h laminates were relatively high when compared with many other natural fibers and petroleum- or bioderived polymer matrix based biocomposites,[23] such as lyocell fiber–PP composites (33.4 MPa),[40] jute fiber–PBS composites (39 MPa),[41] and Kenaf fiber–poly[3-hydroxybutyrate-*co*−3-hydroxyvalerate] composites (16.7 MPa).[42] On the other hand, the flexural strength of these two ACCs were quite low compared to those of an ACC laminate (135.24 MPa) produced from rayon textile by Huber *et al.*[23] with a solvent infusion processing method.[22] However, the values were higher than those of ACC laminates (45 MPa) produced from rayon textile with the prepreg style by Schuermann *et al.*[35]

CONCLUSIONS

In this study, we demonstrated the production of thick ACC laminates using a simple processing route, which was based on hand layup with compressing molding. From this study, it was evident that the process parameters, that is, the dissolution time, pressure, and temperature, had a vital role in controlling the composite structure and properties. The application of pressure during cellulose dissolution and drying helped in controlling the differential shrinkage and void content and also in maintaining the compactness in the lyocell composite laminates. The void content was a key governing factor in controlling the composite stiffness and flexural properties. With a higher dissolution time (3 or 4 h) as the internal voids decreased to a greater extent, the composites showed an improvement in the mechanical properties. The adhesion strength of the lyocell ACCs (especially for LC-3h and LC-4h) was superior to those of most other natural fiber-reinforced composites because of the chemical similarity of the matrix and reinforcing phase in the ACCs. The stiffness of the lyocell ACCs continuously improved with increasing dissolution time as a result of the improved interlaminar adhesion and the reduction of intralaminar and interlaminar voids. The highest tensile strength was achieved with 2 h of dissolution time. The flexural strength of the lyocell ACCs produced with dissolution times of 3 or 4 h were superior to many biocomposites. The repeatability of the tensile test results was found to be very high.

ACKNOWLEDGMENTS

The authors are very grateful to the Aditya Birla Group–Birla Cellulose (Gujrat) for kindly providing the lyocell fabric used in this research. The authors are also thankful to B. L. Deopura (Department of Textile Technology, Indian Institute of Technology Delhi) for his valuable suggestions and technical assistance.

REFERENCES

1. Wu, R. L.; Wang, X. L.; Li, F.; Li, H. Z.; Wang, Y. Z. *Bioresour. Technol.* **2009**, *100*, 2569.
2. John, M. J.; Thomas, S. *Carbohydr. Polym.* **2008**, *71*, 343.
3. Kalia, S.; Dufresne, A.; Cherian, B. M.; Kaith, B. S.; Averous, L.; Njuguna, J.; Nassiopoulos, E. *Int. J. Polym. Sci.* **2011**, *2011*, 1, Article ID 837875.
4. Kabir, M. M.; Wang, H.; Lau, K. T.; Cardona, F. *Compos. B* **2012**, *43*, 2883.
5. Wang, S.; Lin, Y.; Zhang, X.; Lu, C. *RSC Adv.* **2015**, *5*, 50660.
6. Sun, X.; Lu, C.; Liu, Y.; Zhang, W.; Zhang, X. *Carbohydr. Polym.* **2014**, *101*, 642.
7. Qin, C.; Soykeabkaew, N.; Xiuyuan, N.; Peijs, T. *Carbohydr. Polym.* **2008**, *71*, 458.
8. Huber, T.; Pang, S.; Staiger, M. P. *Compos. A* **2012**, *43*, 1738.
9. Ouajai, S.; Shanks, R. A. *Compos. Sci. Technol.* **2009**, *69*, 2119.

10. Bledzki, A. K.; Gassan, J. *Prog. Polym. Sci.* **1999**, *24*, 221.
11. Kalka, S.; Huber, T.; Steinber, J.; Baronian, K.; Mussig, J.; Staiger, M. P. *Compos. A* **2014**, *59*, 37.
12. Pinkert, A.; Marsh, K. N.; Pang, S.; Staiger, M. P. *Chem. Rev.* **2009**, *109*, 6712.
13. Duchemin, B. J. C.; Mathew, A. P.; Oksman, K. *Compos. A* **2009**, *40*, 2031.
14. Kreze, T.; Malej, S. *Text. Res. J.* **2003**, *73*, 675.
15. Bourban, C.; Karamuk, E.; Fondaumiere, M. J. D.; Ruttieux, K.; Mayer, J.; Wintermantel, E. J. *Environ. Polym. Degrad.* **1997**, *5*, 159.
16. Elbadry, E. A.; Aly-Hassan, M. S.; Hamada, H. *Adv. Mech. Eng.* **2012**, *2012*, 1.
17. Lewin, M. Hand Book of Fiber Chemistry, 3rd ed.; CRC: Boca Raton, FL: **2007**; Chapters 9 and 10, p 521.
18. Dube, M.; Blackwell, R. H. In Proceedings of the International Dissolving and Specialty Pulps Conference, Boston, MA, April **1983**; p 111.
19. Fink, H. P.; Weigel, P.; Purz, H. J.; Ganster, J. *Prog. Polym. Sci.* **2001**, *26*, 1473.
20. Isogai, A.; Usuda, M.; Kato, T.; Uryu, T.; Atalla, R. H. *Macromolecules* **1989**, *22*, 3168.
21. Rihm, R. Ph.D. Thesis, Technical University of Berlin, **2003**. http://publica.fraunhofer.de/dokumente/N-29563.html. Accessed 15 June, 2015.
22. Klemm, D.; Heublein, B.; Fink, H. P.; Bohn, A. *Angew. Chem. Int. Ed.* **2005**, *44*, 3358.
23. Huber, T.; Bickerton, S.; Mussig, J.; Pang, S.; Staiger, M. P. *Compos. Sci. Technol.* **2013**, *88*, 92.
24. Pang, J. H.; Liu, X.; Wu, M.; Wu, Y. Y.; Zhang, X. M.; Sun, R. C. *J. Spectrosc.* **2014**, 1.
25. Soykeabkaew, N.; Arimoto, N.; Nishino, T.; Peijs, T. *Compos. Sci. Technol.* **2008**, *68*, 2201.
26. Duchemin, B. J. C.; Newman, R. H.; Staiger, M. P. *Compos. Sci. Technol.* **2009**, *69*, 1225.
27. Zhao, Q.; Yam, R. C. M.; Zhang, B.; Yang, Y.; Cheng, X.; Li, R. K. Y. *Cellulose* **2009**, *16*, 217.
28. Njuhovic, E.; Witt, A.; Kempf, M.; Wolff-Fabris, F.; Glöde, S.; Altstädt, V. *Surf. Coat. Technol.* **2013**, *232*, 319.
29. Tanoglu, M.; Seyhan, A. T. *Int. J. Adhes. Adhes.* **2003**, *23*, 1.
30. Nishino, T.; Peijs, T. In Handbook of Green Materials; Oksman, K., Mathew, A. P., Bismarck, A., Rojas, O., Sain, M., Eds.; World Scientific: Singapore, **2014**; Vol. *2*, Chapter 14, p 201.
31. Huber, T.; Mussig, J.; Curnow, O.; Pang, S.; Bickerton, S.; Staiger, M. P. *J. Mater. Sci.* **2012**, *47*, 1171.
32. Abu-Rous, M.; Ingolic, E.; Schuster, K. C. *Lenzinger Ber.* **2006**, *85*, 31.
33. Abu-Rous, M.; Varga, K.; Bechtold, T.; Schuster, K. C. *J. Appl. Polym. Sci.* **2007**, *106*, 2083.
34. Nishino, T.; Matsuda, I.; Hirao, K. *Macromolecules* **2004**, *37*, 7683.
35. Schuermann, J.; Huber, T.; Staiger, M. P. In Proceedings of ICCM-19 Conference: Canada, Jul–Aug **2013**; p 5626.
36. Afroz, F.; Siddika, A. *Eur. Sci. J.* **2014**, *10*, 202.
37. Haque, M. M. *Daffodil. Int. Univ. J. Sci. Technol.* **2009**, *4*, 62.
38. Awham, M. H.; Zaid, G. M. S. *J. Al-Nahrain Univ.* **2011**, *14*, 58.
39. Carlsson, L. A.; Adams, D. F.; Pipes, R. B. Experimental Characterization of Advanced Composite Materials, 4th ed.; CRC: Boca Raton, FL: **2014**; Chapters 11–15, p 160.
40. Mirza, F. A.; Rasel, S. M.; Kim, M. S.; Afsar, A. M.; Kim, B. S.; Song, J. *Adv. Mater. Res.* **2010**, *123*, 1159.
41. Liu, L.; Yu, J.; Cheng, L.; Qu, W. *Compos. A* **2009**, *40*, 669.
42. Persico, P.; Acierno, D.; Carfagna, C.; Cimino, F. *Int. J. Polym. Sci.* **2011**, *1*, Article ID 841812.